Journal of Sound and Vibration (1989) **135**(3), 399-410

FREE OSCILLATIONS OF A CAVITATION BUBBLE

K. VOKURKA†

Department of Physics, Faculty of Electrical Engineering, Czech Technical University, Suchbátarova 2, CS-166 27 Praha 6, Czechoslovakia

(*Received* 6 *September* 1988, *and in revised form* 30 *March* 1989)

A cavitation bubble model based on a recently described vapour bubble model is presented. By using the model, significant bubble wall positions and related quantities are computed. Experimental data on cavitation bubbles as published in the literature are evaluated and compared with the theoretical results. It is found that, in agreement with an assumption made, at later times the cavitation bubbles behave similarly to spark- and laser-generated bubbles. The difference in the computed and measured values of the cavitation bubble damping factors are interpreted as extra energy losses. The mechanism of these losses is, however, still unclear. Possible origins of the losses are suggested.

1. INTRODUCTION

When the pressure in a real liquid is reduced below a certain critical value, the liquid begins to evaporate into ever-present nuclei, thus forcing them to grow. After the pressure has been re-increased above the critical value, the vapour bubbles formed around the nuclei begin to collapse and perform several damped free oscillations. This phenomenon is called cavitation and has many important consequences for fluid engineering [1].

In this paper the behaviour of a single spherical cavitation bubble oscillating in a liquid far from boundaries is analyzed. For this purpose a simple yet sufficiently accurate bubble model is introduced. To simplify the theoretical analysis further, only medium-sized bubbles are considered, for which the size-dependent effects such as gravity, surface tension, viscosity and heat conduction can be neglected. (Whereas omission of gravity, surface tension and viscosity from the analysis is fully justified in the case of experimental cavitation bubbles, this unfortunately cannot be said about heat conduction.) The experimental data published by Knapp and Hollander [2], Chesterman [3], Schmid [4], Gallant [5], Blake *et al.* [6], Fujikawa and Akamatsu [7], and Bark and van Berlekom [8] are evaluated and compared with the theoretical results.

2. CAVITATION BUBBLE MODEL

Let a spherical cavitation nucleus of a radius R_n be exposed at a time $t=0$ to an instantaneous pressure reduction Δp. If the initial ambient pressure in the liquid is denoted as $p_{\infty i}$, then the new ambient pressure will be $p_{\infty d} = p_{\infty i} - \Delta p$. Let us assume that $p_{\infty d} < P_v$, where P_v is the liquid vapour pressure for a given liquid temperature. Due to the pressure reduction mentioned above the liquid begins to evaporate into the nucleus, thus keeping the pressure inside the nucleus equal to P_v. However, as the pressure inside the nucleus is larger than the ambient pressure $p_{\infty d}$, the nucleus starts to grow. (Here we assume only moderate pressure reductions Δp so that evaporation keeps pace with the nucleus growth.)

†Present address: Švédská 27, CS-466 01 Jablonec n.N., Czechoslovakia.

0022-460X/89/240399+12 $03.00/0

Let the pressure reduction last for a time ΔT (the so-called *driving phase*). During the interval ΔT the nucleus steadily grows and converts into a visible vapour bubble. At the same time the surrounding liquid acquires kinetic energy. At a time $t = \Delta T$ let the ambient pressure be raised to a value $p_{\infty c} > P_v$. As a consequence the rate of the bubble growth slows down. However, the bubble still continues to grow until the kinetic energy of the liquid (aquired during the driving phase) is expended in working against the pressure difference $p_{\infty c} - P_v$. The bubble wall motion stops at a maximum radius, R_{M1}. During this prolonged growth evaporation of the liquid into the bubble interior continues because the bubble expansion causes the pressure at the bubble wall, P, to drop below the value of P_v. Hence it can be assumed that for the whole *growth phase* $P = P_v$. The growth phase lasts a time T_g.

After reaching the maximum radius, R_{M1}, the bubble wall motion reverts and the bubble enters a phase known as the bubble collapse. At the beginning of the *collapse phase*, which lasts a time T_c, condensation manages to maintain the equality $P = P_v$. However, as the wall velocity increases, condensation ceases to keep pace with the wall motion and the vapour remaining in the bubble starts to behave as a non-condensable gas. The pressure increase in the compressed vapour will eventually stop the inward wall motion at a minimum radius, R_{m1}; the wall motion then reverts and the bubble enters a phase known as the *rebound phase*. During the rebound phase the bubble grows to a maximum radius R_{M2} and then again collapses. The collapse and rebound phases recur several times during the bubble life.

As shown in reference [9] the *bubble wall motion* can often be described with sufficient accuracy by the modified Herring's equation

$$\ddot{R}R + \tfrac{3}{2}\dot{R}^2 = (1/\rho_\infty)[P - p_\infty + \dot{P}R/c_\infty]. \tag{1}$$

Here R is the bubble radius, ρ_∞ is the liquid density, p_∞ is the time-varying ambient pressure, c_∞ is the speed of sound in the liquid, and the overdots denote differentiation with respect to time.

As discussed above, it is assumed that during the *growth phase* the pressure at the bubble wall equals the vapour pressure:

$$P = P_v. \tag{2}$$

For the *driving phase* ($0 \leq t \leq \Delta T$) equation (1) has a simple solution [10],

$$\dot{R}^2 = \tfrac{3}{2}(1/\rho_\infty)(P_v - p_{\infty d})[1 - (R_n/R)^3], \tag{3}$$

which for R larger than a few nucleus radii R_n can be simplified by omitting the second term in the square brackets.

The bubble *collapse* and *rebound* can be conveniently described by a simple model given in reference [11]. In this model, for wall velocities lower than a certain transition velocity, $\dot{R}_{vg}$, the bubble is assumed to behave as an *ideal vapour bubble* (at which condensation and evaporation take place at an infinite speed), and for wall velocities higher than $\dot{R}_{vg}$, as an *ideal gas bubble* (at which condensation and evaporation are zero). Hence one can write

$$P = \begin{cases} P_v, & |\dot{R}| < |\dot{R}_{vg}|, \quad R > R_{vg} \\ P_v(R/R_{vg})^{3\gamma}, & |\dot{R}| \geq |\dot{R}_{vg}|, \quad R \leq R_{vg} \end{cases}. \tag{4}$$

Here R_{vg} is the radius at which the bubble changes its behaviour, and γ is the polytropic exponent of the vapour. The values of the transition velocity and of the polytropic exponent then determine the intensity of bubble oscillations.

An oscillating bubble radiates *pressure waves* into the surrounding liquid. The pressure wave, p_a, at a point in the liquid, r, can be determined to a first approximation by a simple formula ($r \gg R$)

$$p_a = (P - p_\infty + \tfrac{1}{2}\rho_\infty \dot{R}^2) R/r. \tag{5}$$

The cavitation bubble model presented here is thus given by equations (1), (2), (4) and (5). To solve these equations it is sufficient to know (in addition to the physical constants) just the form of the variable ambient pressure $p_\infty(t)$. Note that equation (1) could be easily replaced by a more sophisticated equation of motion, such as Gilmore's. However, in this paper the intensity of cavitation bubble oscillations will be assumed to be such that no substantial improvements in the model performance would be obtained.

The reader is recommended to compare this cavitation bubble model with a similar model of spark- and laser-generated bubbles given in reference [12]. The latter model is also based on the vapour bubble equation (4). However, an important distinction (in addition to the form of the pressure $p_\infty(t)$) is in the equation describing the pressure at the bubble wall during the bubble growth (equation (2)). Thus by connecting the vapour bubble equation (4) with a suitable equation for the growth phase either the cavitation bubble model or the spark- and laser-generated bubble model were obtained. It should be also noted that in the literature often no distinction is made between these bubbles, all being called cavitation bubbles. Oscillations of these bubbles are then usually computed for wall motions beginning at the first maximum radius R_{M1}, and this unfortunately is done even in those situations where inclusion of earlier bubble histories in computations could provide very valuable information. It is hoped that introduction of the complete model here could help to overcome the traditional approach.

3. RESULTS OF COMPUTATION

Before starting computations it is convenient to introduce the *non-dimensional* system of *Y-variables*:

$$t_y = t/[R_n(\rho_\infty/p_{\infty i})^{1/2}], \qquad Y = R/R_n, \qquad P^* = P/p_{\infty i},$$

$$p_{ya} = (p_a/p_{\infty i})r/R_n, \qquad c_\infty^* = c_\infty(\rho_\infty/p_{\infty i})^{1/2}.$$

Computations will be performed for the following values of the *physical constants* (water under ordinary laboratory conditions):

$$p_{\infty i} = 100\ \text{kPa}, \qquad \rho_\infty = 10^3\ \text{kg m}^{-3}, \qquad c_\infty = 1450\ \text{m s}^{-1},$$

$$P_v = 2\ \text{kPa}, \qquad |\dot{R}_{vg}| = 6\ \text{m s}^{-1}, \qquad \gamma = 1{\cdot}25.$$

Here the values of the transition velocity, $\dot{R}_{vg}$, and of polytropic exponent, γ, were determined in reference [11] by comparison of calculated and measured peak pressures in the bubble pulses, the experimental data originating from spark-generated bubbles. Using these values in this paper then implies that the same intensity of oscillations is assumed both for spark-generated and cavitation bubbles.

An example of the computed bubble wall motion time history is displayed in Figure 1, and of the radiated pressure wave in Figure 2. The computed significant bubble wall positions are given in Table 1. From the computed significant bubble wall positions a number of related quantities were determined: these are summarized in Table 2. computations were performed by using the normalized form of equations (1), (2), (4) and (5),

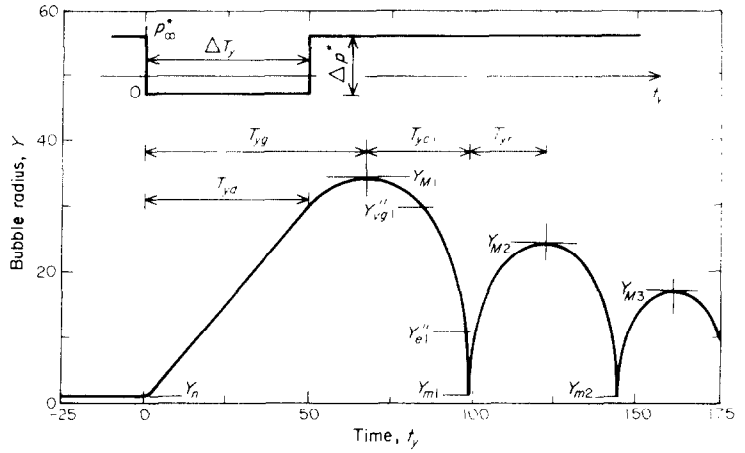

Figure 1. Computed time history of the cavitation bubble wall motion. T_{ya}, time of the driving phase; T_{yg}, time of the bubble growth; T_{yc1}, time of the first bubble collapse; T_{yr1}, time of the first bubble rebound.

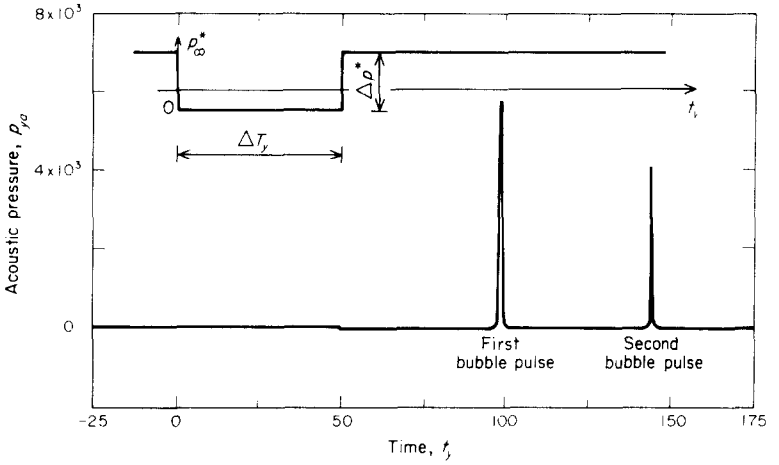

Figure 2. Computed pressure wave radiated by an oscillating cavitation bubble.

TABLE 1

Computed significant bubble wall positions of the cavitation bubble

Y_n	Y_{M1}	Y''_{vg1}	Y''_{e1}	Y_{m1}	Y'_{e2}	Y'_{vg2}	Y_{M2}	Y''_{vg2}	Y''_{e2}	Y_{m2}	Y'_{e3}	Y'_{vg3}	Y_{M3}
1	34·42	29·74	10·48	1·06	10·48	21·08	24·40	21·08	7·43	0·75	7·43	14·94	17·30

TABLE 2

Computed significant bubble wall positions, amplitudes of oscillations, peak pressures in the bubble pulses, and damping factors of the cavitation bubble

Z''_{vg1}	A''_1	Z_{m1}	p_{zp1}	A'_2	Z'_{vg2}	α_1	Z''_{vg2}	A''_2	Z_{m2}	p_{zp2}	A'_3	Z'_{vg3}	α_2
0·86	3·29	0·03	167	2·33	0·86	0·71	0·86	3·29	0·03	167	2·33	0·86	0·71

and for the ambient pressure change shown in Figures 1 and 2, where $\Delta T_y = 50$, $\Delta p^* = -1{\cdot}5$ and $p^*_{\infty i} = p^*_{\infty} = 1$.

In Table 1, Y_M denotes the maximum bubble radius, Y_{vg} the "transition" radius, Y_e the equilibrium radius (determined from the condition that $P^* = p^*_{\infty c}$ when $Y = Y_e$) and Y_m the minimum radius. The quantities belonging to the collapse phases are denoted by two primes and those belonging to the rebound phases by one prime.

The quantity Y_{M1} will be referred to as the *growth factor.* It represents the size that the bubble attains during the growth phase. The value of the growth factor is determined by the form of the ambient pressure change $p_{\infty}(t)$. For particular experimental conditions it is a constant. In real liquids the size of nuclei is usually of the order of 10^{-6} m and the size of cavitation bubbles of the order of 10^{-3} m. Hence the typical growth factor is of the order of 10^3. (For practical reasons a much smaller growth factor was selected for the example.)

For easier interpretation of the results some quantities in Table 2 are given in the Z-system of the non-dimensional variables. These are the radii $Z''_{vg1} = R''_{vg1}/R_{M1}$, $Z'_{vg2} = R'_{vg2}/R_{M2}$, $Z''_{vg2} = R''_{vg2}/R_{M2}$, $Z'_{vg3} = R'_{vg3}/R_{M3}$, $Z_{m1} = R_{m1}/R_{M1}$, $Z_{m2} = R_{m2}/R_{M2}$, and the peak pressures in the bubble pulses $p_{zp1} = (P^*_{M1} - 1)Z_{m1}$, and $p_{zp2} = (P^*_{M2} - 1)Z_{m2}$. (Here P^*_M is the maximum pressure at the bubble wall: i.e., $P^*_M = P^*_v(Z_{vg}/Z_m)^{3\gamma}$.)

The amplitudes of the bubble oscillations, A, are defined in the following way: $A''_1 = R_{M1}/R''_{e1}$, $A'_2 = R_{M2}/R'_{e2}$, $A''_2 = R_{M2}/R''_{e2}$ and $A'_3 = R_{M3}/R'_{e3}$. Similarly, the damping factors, α, are defined as follows: $\alpha_1 = R_{M2}/R_{M1}$, $\alpha_2 = R_{M3}/R_{M2}$.

Note that the rebound amplitudes, A'_2, A'_3, ..., represent the amplitudes for which the bubble would be excited, if it were a gas bubble. These amplitudes are in essence determined by the maximum pressures, P^*_M. However, due to the collapse mechanism the collapse amplitudes A''_1, A''_2, ..., are larger than the rebound ones. Note also that for the computational model considered it holds that $A'_2 = A'_3 = \cdots$, $A''_1 = A''_2 = \cdots$, $\alpha_1 = \alpha_2 = \cdots$, $P^*_{M1} = P^*_{M2} = \cdots$, $p_{zp1} = p_{zp2} = \cdots$, $Z''_{vg1} = Z'_{vg2} = Z''_{vg2} = \cdots$, and $Z_{m1} = Z_{m2} = \cdots$. As could be expected (because of the same vapour bubble model employed), these results are the same as those obtained for spark- and laser-generated bubbles. For a more detailed discussion of these relations the reader is therefore referred to the earlier paper [12].

4. EVALUATION OF EXPERIMENTAL DATA

In this section it is intended to evaluate some of the experimental data found in the literature and to compare them with the cavitation bubble model results presented above. As far as the author is aware, similar evaluation of experimental data on the cavitation bubbles has not been published previously in the literature.

An important prerequisite for the cavitation inception is the existence of cavitation nuclei in the liquid. As the nuclei are distributed in the liquid at random and as their size is also random, the resulting cavitation always has a random character. This makes direct observation of cavitation bubbles extremely difficult. As a consequence, very few experimental investigations of real cavitation bubbles have been reported so far, and in these investigations only a limited number of bubbles and bubble parameters have been studied. Naturally, evaluation of limited data can yield only limited results.

The dynamic ambient pressure reduction necessary for cavitation bubble generation can experimentally be achieved in two ways. First, cavitation can occur in a flowing stream or on moving bodies. The method producing cavitation bubbles in a flowing stream was used, e.g., by Knapp and Hollander [2], Blake *et al.* [6], and Bark and van Berlekom [8]. Second, the necessary pressure reduction can be achieved by a tension pulse which

propagates through the liquid. This technique was used, e.g., by Chesterman [3], Schmid [4], Gallant [5], and Fujikawa and Akamatsu [7]. A review of the generation of tension in liquids was also recently given by Trevena [13]. In real environments the changes of the ambient pressure never have the simple square form shown in Figures 1 and 2. Rather, the pressure $p_\infty(t)$ continuously varies during the bubble life and the particular shape of the ambient pressure field is determined by the particular experimental arrangement.

As discussed in detail in reference [14], as many quantities as possible should be measured if one wants to arrive at a solid interpretation of the experimental data in bubble dynamics. The measured quantities can be, for example, a succession of the maximum bubble radii R_{M1}, R_{M2}, $R_{M3}, \ldots$, the collapse times T_{c1}, $T_{c2}, \ldots$, the peak pressures in the bubble pulsar p_{p1}, p_{p2}, 0, and the effective widths of the bubble pulses ϑ_1, $\vartheta_2, \ldots$.

The basic method of investigation used by all the authors mentioned above is high-speed photography of the bubble oscillations. Some authors, as for example Gallant [5], Fujikawa and Akamatsu [7], and Bark and van Berlekom [8], have also recorded the pressure variations in the liquid (usually the changes of the ambient pressure with superimposed bubble pulses radiated by the oscillating bubbles). However, these pressure records, although extremely useful for determining the details of the pressure field $p_\infty(t)$, do not allow one to determine such useful quantities as the peak pressure in the bubble pulse and the effective width of the bubble pulse. Thus from those quantities mentioned above the only ones that can be used for the evaluation here are the first and second maximum bubble radii R_{M1} and R_{M2}, the first collapse time T_{c1}, and in some cases also the third maximum radius R_{M3}, all these quantities being determined by high-speed photography as mentioned.

Some authors (e.g., Chesterman [3], Schmid [4], and Bark and van Berlekom [8]) have not reported the form of the variable pressure field $p_\infty(t)$ in their experiments. In these cases, however, the ambient pressure $p_{\infty c}$ (more exactly, the "average" pressure during the collapse phase) can be determined, by using the values of R_{M1} and T_{c1}, from Rayleigh's formula for the collapse time of a vapour bubble: i.e.,

$$p_{\infty c} = \rho_\infty (R_{M1} T_{zc1v} / T_{c1})^2 + P_v. \tag{6}$$

Here $T_{zc1v} \doteq 0{\cdot}92$ is the collapse time of the vapour bubble in the Z-system of the non-dimensional variables, and this collapse time can be shown to vary only very little with $p_{\infty c}$ [15]. (Note that the non-dimensional collapse time shown in Figure 8 in reference [15] is defined as $T_{zc1} = T_{c1}/[R_{M1}(\rho_\infty/p_{\infty c})^{1/2}]$. A mutual realtion between the two non-dimensional collapse times is then $T_{zc1v} = T_{zc1}(1 - P_v/p_{\infty c})^{1/2}$. After substituting the values of T_{zc1} corresponding to different ambient pressures $p_{\infty c}$ into this formula, validity of the claim that T_{zc1v} is independent of $p_{\infty c}$ can easily be verified.)

The formula (6) was tested first by means of data from experiments where the pressure $p_{\infty c}$ was known (see, e.g., Figures 7 and 9 in reference [2], and Figures 3, 4 and 15 in reference [5]). Having been found satisfactory, it was used afterwards for calculating the pressure $p_{\infty c}$ in those cases where the ambient pressure was not given explicitly in the reports. However, let us note here that in some cases the application of formula (6) to experimental data led evidently to incorrect results (as, e.g., in the case of Figure 8 in reference [2]).

From the measured maximum radii it was possible to determine the first damping factor, α_1, and in some cases also the second damping factor, α_2. These damping factors together with the corresponding bubble-sizes, R_{M1}, and the ambient pressures, $p_{\infty c}$, (as determined from the formula (6)) are summarized in Table 3. Variations of the first damping factor with the bubble size and the ambient pressure, respectively, are shown

TABLE 3

Experimental data on cavitation bubbles; *notes*: †, *the value of* $p_{\infty c}$ *was estimated from the published form of the ambient pressure field* $p_\infty(t)$; ‡, *the value of* $p_{\infty c}$ *was computed from data given in the caption to Figure* 13 *of reference* [6] *by using an estimated value of the pressure coefficient*: $C_p = -0{\cdot}15$

Source of data							
Authors	Figure	Further descriptors	R_{M1} (mm)	$p_{\infty c}$ (kPa)	α_1 (−)	α_2 (−)	Symbols in Figures 3–5
Knapp and Hollander [2]	7		3·8	21·2	0·70	0·75	×
	9		3·6	20·9	0·86	0·77	⊕
Chesterman [3]	2(a)		6·8	2·5	0·74	0·67	○
	2(b)		4·0	4·2	0·85	0·55	●
	2(c)		6·9	3·6	0·77	0·67	⊙
	3(c)	Strip no. 39	6·6	2.4	0·47		▲
	3(c)	Strip no. 40	6·9	2·3	0·69		▽
	3(c)	Strip no. 41	6·1	2·4	0·43		◇
	3(c)	Strip no. 42	6·1	2·2	0·51		◆
Schmid [4]	2		5·8	14·8	0·50		△
Gallant [5]	11	Curve no. 2	2·0	~2·5†	0·56	0·55	□
	11	Curve no. 3	2·5	~2·5†	0·70	0·71	■
Blake *et al.* [6]	13		6·4	~8·5‡	0·66		⧓
Fujikawa and Akamatsu [7]	8		1·0	71·2	0·38		▼
Bark and van Berlekom [8]	24		3·6	5·5	0·49		⊠
Average values			4·8	11·1	0·62	0·67	

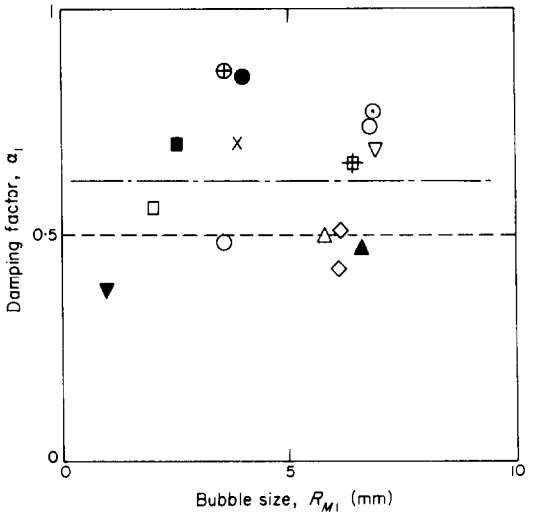

Figure 3. Variation of the first damping factor, α_1, with the bubble size, R_{M1}. — · —, Average value for cavitation bubbles, - - - average value for spark- and laser-generated bubbles. See Table 3 for key.

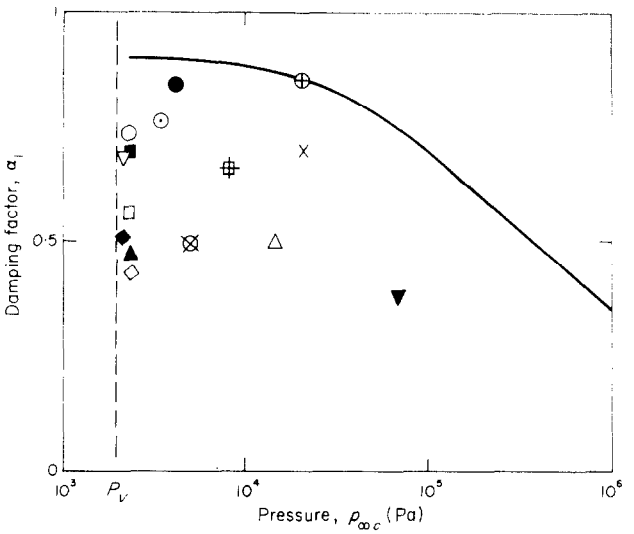

Figure 4. Variation of the first damping factor, α_1, with the ambient pressure, $p_{\infty c}$. ——, Theoretical curve. See Table 3 for key.

in Figures 3 and 4. Variation of the second damping factor with the bubble size is given in Figure 5. Also displayed in Figure 4 is a theoretical variation of α_1 with $p_{\infty c}$ as computed for the medium-sized vapour bubbles in reference [15, Figure 11]. Unfortunately, no such theoretical variation of α_1 with R_{M1} is known for vapour bubbles at present, although for bubble sizes considered, i.e., for R_{M1} ranging from 1 to 10 mm, the bubble behaviour is strongly influenced by heat losses [16] and thus, in theory at least, α_1 should vary with R_{M1}.

It was shown elsewhere [14] that knowledge of one non-dimensional quantity only is insufficient for determining the amplitudes of bubble oscillations A_1, $A_2, \ldots$, and for

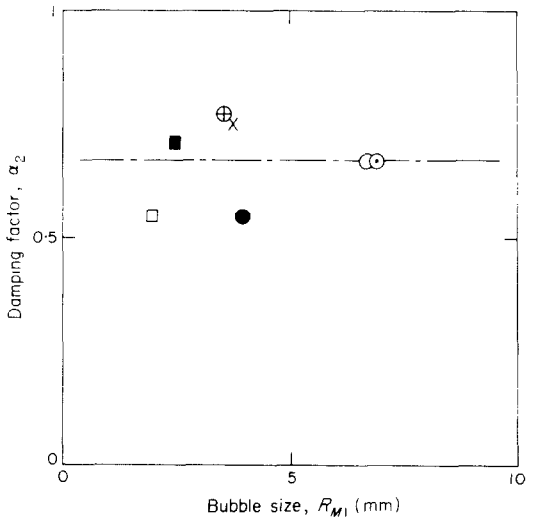

Figure 5. Variation of the second damping factor, α_2, with the bubble size, R_{M1}. — · —, Average value. See Table 3 for key.

validation of the theoretical model. Unfortunately, in the case of the cavitation bubbles only the damping factors α_1 and α_2 are known. Thus it cannot be verified completely convincingly whether or not the cavitation bubbles really behave for $t > T_g$ like the spark- and laser-generated bubbles (this assumption has been used, for example, in section 2 when formulating the cavitation bubble model). Nevertheless, the comparison of available data shows that at least as far as the damping factor α_1 is concerned these bubbles behave similarly.

With respect to the limited data base it is highly useful to have a brief look at the results obtained in references [14, 16, 17], where data from experiments with bubbles generated by underwater explosions, sparks and lasers were analyzed. In these references, when applying the theoretical model to experimental data, one could choose agreement either in the value of the first minimum radius R_{m1} (represented by the measured peak pressure p_{p1}) or in the value of the second maximum radius R_{M2} (represented by the measured damping factor α_1). However, it was not possible to obtain agreement in both p_{p1} and α_1 at the same time. For reasons discussed in great detail in the references mentioned, it was decided to accept the agreement in p_{p1} and to reject that in α_1, thus accepting the idea of an additional damping.

To return to the present problem, when comparing the damping factor α_1 in experiments with spark- and laser-generated bubbles with data given in Figures 3–5 one can notice, first, that the damping factors are approximately the same (the difference in the average value is discussed later). The damping factors are also often much smaller than those on the theoretical curve given in Figure 4. This indicates that, similarly as in the case of bubbles generated by underwater explosions, sparks and lasers, there is an additional dissipative mechanism not accounted for in the theoretical model. In the case of cavitation bubbles considered here this mechanism may be, in part, heat conduction. However, heat conduction alone cannot explain all the energy losses [16]. Therefore further mechanisms must be considered. Possible mechanisms, as suggested by various researches, were reviewed in reference [17]. They may be briefly summarized as follows: (i) turbulence in the water surrounding the bubble induced by the bubble wall distortion; (ii) loss of gas from the main bubble in the form of microbubbles; (iii) excessive gas cooling in the protuberances; (iv) internal converging shocks.

The data given in Figures 3 and 5 also seem to support an earlier finding [16] that the damping factors α_1 and α_2 are independent of the bubble size, R_{M1}, even in the region where heat losses are significant: i.e., for R_{M1} ranging from 1 to 10 mm (certainly, more data are needed to answer this question with greater confidence). As far as the variation of α_1 with $p_{\infty c}$ is concerned, the data given in Figure 4 are insufficient to allow one to draw any more serious conclusions (there is only one measured point for the pressure region $p_{\infty c} > 22$ kPa, where the theoretical curve starts decreasing significantly).

Finally, the data points show a very large scatter. Similar scatter was also found in the case of the damping factors of spark- and laser-generated bubbles. It indicates the presence of a dissipative mechanism acting in a random manner and thus it supports the suspicion that the primary cause of the extra energy losses is the bubble wall distortion, which is always irregular (and random).

As mentioned above, in some cases it was also possible to determine the value of the second damping factor, α_2. In theory, α_2 should equal α_1 (cf. Table 2). However, as can be seen from Table 3, in real situations three cases can occur. These are as follows.

(i) $\alpha_1 < \alpha_2$. Such a damping, which represents a decrease of energy dissipated in the second period of bubble oscillation as compared with the first period is typical for gas bubbles. In the case of the vapour bubbles this damping may indicate rectified diffusion of dissolved gases from the liquid into the bubble interior.

(ii) $\alpha_1 = \alpha_2$. This represents an equal damping for the first and second bubble oscillations. Such a damping is predicted by the simple vapour bubble model given in section 2.

(iii) $\alpha_1 > \alpha_2$. This represents an increase in the damping for the second bubble oscillation. The increased damping can be attributed to the stronger influence of the yet unknown dissipative mechanism (most probably turbulence) and to the size-dependent effects, such as viscosity and heat conduction, also not accounted for in the model.

If one computes the average values of the damping factors in Table 3, then these are $\langle\alpha_1\rangle = 0{\cdot}62$ and $\langle\alpha_2\rangle = 0{\cdot}67$. If the influence of $p_{\infty c}$ and R_{M1} on the damping is disregarded for a moment, then the difference in these averages indicates that there is a net increase of the non-condensable gas in the bubble interior (due to the rectified diffusion) during the bubble oscillations.

The average damping factor as found for spark- and laser-generated bubbles in reference [16] is $\langle\alpha_1\rangle = 0{\cdot}5$. The reason why the average damping factor of cavitation bubbles rates higher is, most probably, the lower average value of the ambient pressure. Whereas in experiments with spark- and laser-generated bubbles the ambient pressure was $p_{\infty c} = 100$ kPa, the average value of the ambient pressures given in Table 3 is $\langle p_{\infty c}\rangle = 11{\cdot}4$ kPa. Let us note that the theoretical difference in α_1 for the two pressures is $(\Delta\alpha_1)_{theor.} = 0{\cdot}88 - 0{\cdot}71 = 0{\cdot}17$ (see Figure 4). This compares quite favourably with the experimental difference $(\Delta\alpha_1)_{exp.} = 0{\cdot}62 - 0{\cdot}5 = 0{\cdot}12$.

5. DISCUSSION AND CONCLUSION

For a known form of the ambient pressure field $p_\infty(t)$, the cavitation bubble model introduced in section 2 makes it possible to compute the bubble wall time history, $R(t)$, and the radiated pressure wave, $p_a(t)$, both with relative ease and sufficient accuracy. This should be convenient for experimentalists, first of all, who often have no time to use advanced (and complicated) models described in the literature from time to time and resort to a much less accurate approach based on modeling the vapour bubble by gas bubble. In this respect the model presented here is a step forward because by retaining the simplicity of the gas bubble approximation it makes it possible to incorporate some features not accessible for gas bubble approximation.

Evaluation of the available experimental data on cavitation bubbles and their comparison with analogous data on spark- and laser-generated bubbles indicate that the model yields satisfactory predictions up to the time of the first bubble collapse: i.e., in the time interval $\langle 0, T_g + T_{c1}\rangle$. At later stages in real bubbles large energy losses occur, not covered up by the model. For the range of bubble sizes examined in this study these losses are partially due to heat conduction. However, the mentioned comparison with other experiments reveals that there are further dissipative mechanisms, and these seem to be even more important than heat conduction. Unfortunately, the nature of these mechanisms has not been clarified yet. Among possible candidates are turbulence, excessive heat and gas losses from the bubble (all these three mechanisms could be provoked by the bubble wall distortion), and converging shocks in the bubble interior. Examination of the damping factor data also indicates that the unknown dissipative mechanism acts partially in a random manner. This only further supports the idea that the primary cause of the extra losses is the irregular bubble wall distortion observed during the real bubble oscillations.

The model accuracy would be increased if rectified gas diffusion from the liquid into the bubble interior were included. Finally, the use of the transition condition $\dot{R} = \dot{R}_{vg}$ for the rebound phases is not quite correct, but it is hoped that the error thus introduced is small.

It is evident that only further experiments can throw more light on the complicated behaviour of real cavitation bubbles. In this connection it should be emphasized that significant progress can be achieved only if the high-speed photography methods are supplemented by detailed bubble pulse measurements as discussed elsewhere [14].

When formulating the cavitation bubble model in section 2, the assumption was made that the wall velocity during the driving phase is sufficiently low (e.g., $\dot{R} < 6\ \mathrm{m\,s^{-1}}$). Examination of the available experimental records shows that this is also the case with real cavitation bubbles (see, e.g., Figures 8 and 9 in reference [2], and Figure 8 in reference [7]). With respect to these low-growth velocities it is felt that the designation of the cavitation bubble growth as "explosive" (see, e.g., reference [1], page 1) is inadequate. On the contrary, the growth velocities of the cavitation bubbles are approximately two orders lower than the growth velocities of the explosion, spark- and laser-generated bubbles or the collapse velocities of any vapour bubble [14, 16, 17].

In the literature the possibility of complete bubble break-up into many very minute bubbles has sometimes been mentioned (see, e.g., references [18, 19]). Such a break-up may be a source of an intense turbulence and increased cooling of the minute bubbles, but it cannot prevent the bubble from rebounding. The compressed vapour will force the minute bubbles to grow and later to coalesce into a larger bubble. Due to increased energy dissipation the regrown bubble may be of smaller size than it would be if the break-up did not occur. The collapse without visible rebound, as reported by Harrison [20], who observed only grey fog after the bubble collapse, seems highly improbable, if not impossible on physical grounds. (Occurrence of just the grey fog formed by many quiescent minute bubbles would require that all the liquid kinetic energy associated with the radial flow be dissipated during the collapse phase and none be transferred into the internal energy of the vapour. However, if that were possible at all, then there would be no reasons for the bubble to disintegrate because after reaching the minimum volume the bubble would cease to perform any movement.)

In the literature the pressure pulses radiated by the cavitation bubbles are usually called the "shock waves". However, such a term is questionable since the existence of the shock fronts in the leading edge of the pressure pulses and the associated supersonic velocities of the pulses have never been experimentally proved. On the contrary, the few investigations that have been carried out revealed almost sonic velocities of the pressure pulses [21], their smooth profiles (see, e.g., Figure 3 in reference [22] and Figure 10 in reference [23]), and their acoustic propagation ($1/r$ law)—see, e.g., Figure 5 in reference [24] and Figure 5 in reference [25]. Thus, until further experimental evidence proves the contrary, it seems more appropriate to use the more moderate term "bubble pulse" even in the case of cavitation bubbles (the term "bubble pulse" was originally coined in underwater explosions research—see reference [26]).

REFERENCES

1. R. T. KNAPP, J. W. DAILY and F. G. HAMMITT 1970 *Cavitation.* New York: McGraw-Hill.
2. R. T. KNAPP and A. HOLLANDER 1948 *Transactions of the American Society of Mechanical Engineers* **70**, 419-431. Laboratory investigations of the mechanism of cavitation.
3. W. D. CHESTERMAN 1952 *Proceedings of the Physical Society (London)* **B65**, 846-858. The dynamics of small transient cavities.
4. J. SCHMID 1959 *Acustica* **9**, 321-326. Cinematographical investigation of single-bubble cavitation (in German).
5. H. GALLANT 1962 *Österreichische Ingenieur-Zeitschrift* **5**, 74-83. Investigations of cavitation bubbles (in German).
6. W. K. BLAKE, M. J. WOLPERT and F. E. GEIB 1977 *Journal of Fluid Mechanics* **80**, 617-640. Cavitation noise and inception as influenced by boundary-layer development on a hydrofoil.

7. S. FUJIKAWA and T. AKAMATSU 1978 *Bulletin of the Japan Society of Mechanical Engineers* **21**, No. 152, 223-230. Experimental investigations of cavitation bubble collapse by a water shock tube.
8. G. BARK and W. B. VAN BERLEKOM 1979 *Publication of the Swedish State Shipbuilding Experimental Tank No.* 83, *Göteborg.* Experimental investigations of cavitation dynamics and cavitation noise.
9. K. VOKURKA 1986 *Acustica* **59**, 214-219. Comparison of Rayleigh's, Herring's and Gilmore's models of gas bubbles.
10. M. S. PLESSET 1957 in *Proceedings of the 1st Symposium on Naval Hydrodynamics* (S. Sherman, editor), 297-318. Washington: National Academy of Sciences. Physical effects in cavitation and boiling.
11. K. VOKURKA 1987 *Journal of the Acoustical Society of America* **81**, 58-61. A simple model of a vapor bubble.
12. K. VOKURKA 1988 *Czechoslovak Journal of Physics* **B38**, 27-34. A model of spark and laser generated bubbles.
13. D. H. TREVENA 1984 *Journal of Physics D* **17**, 2139-2164. Cavitation and the generation of tension in liquids.
14. K. VOKURKA 1986 *Czechoslovak Journal of Physics* **B36**, 600-615. A method for evaluating experimental data in bubble dynamics studies.
15. K. VOKURKA 1988 *Journal of Sound and Vibration* **126**, 73-83. Influence of the ambient pressure on free oscillations of bubbles in liquids.
16. K. VOKURKA 1988 *Czechoslovak Journal of Physics* **B38**, 35-46. Evaluation of data from experiments with spark and laser generated bubbles.
17. K. VOKURKA 1987 *Acta Technica ČSAV* **32**, 162-172. Oscillations of gas bubbles generated by underwater explosions.
18. M. S. PLESSET 1974 in *Finite-Amplitude Wave Effects in Fluids* (L. Bjørnø, editor), 203-209. Guildford: IPC Science and Technology Press. Bubble dynamics and cavitation erosion.
19. A. PROSPERETTI and A. LEZZI 1986 *Journal of Fluid Mechanics* **168**, 457-478. Bubble dynamics in a compressible liquid. Part 1. First-order theory.
20. M. HARRISON 1952 *Journal of the Acoustical Society of America* **24**, 776-782. An experimental study of single bubble cavitation noise.
21. A. SHIMA, K. TAKAYAMA, Y. TOMITA and N. MIURA 1981 *Acustica* **48**, 293-301. An experimental study on effects of a solid wall on the motion of bubbles and shock waves in bubble collapse.
22. H. KUTTRUFF and U. RADEK 1969 *Acustica* **21**, 253-259. Measurements of the pressure contours in pressure pulses generated by cavitation (in German).
23. Y. TOMITA and A. SHIMA 1986 *Journal of Fluid Mechanics* **169**, 535-564. Mechanisms of impulsive pressure generation and damage pit formation by bubble collapse.
24. A. SHIMA, K. TAKAYAMA, Y. TOMITA and N. OHSAWA 1983 *AIAA Journal* **21**, 55-59. Mechanism of impact pressure generation from spark-generated bubble collapse near a wall.
25. A. SHIMA, Y. TOMITA and K. TAKAHASHI 1984 *Proceedings of the Institution of Mechanical Engineers* **198C**, 81-86. The collapse of a gas bubble near a solid wall by a shock wave and the induced impulsive pressure.
26. R. H. COLE 1948 *Underwater Explosions.* Princeton, New Jersey: Princeton University Press.